BUTTERWORTH HEINEMANN

Polymer Vol. 36 No. 11, pp. 2115-2121, 1995

0032-3861/95/$10.00+0.00

polymer papers

The structure of highly textured quasi-single-crystalline high-density polyethylene probed by atomic force microscopy and small-angle X-ray scattering

H. Schönherr and G. J. Vancso*
University of Toronto, Department of Chemistry, 80 St George Street, Toronto, Ontario M5S 1A1, Canada

and A. S. Argon
Massachusetts Institute of Technology, Cambridge, MA 02139, USA
(Received 28 July 1994; revised 15 November 1994)

Previous texture evolution experiments carried out on high-density polyethylene to an equivalent strain of $\varepsilon_e = 1.86$ have indicated the development of a quasi-single-crystalline long-range coherence in the principal direction of molecular alignment parallel to the direction of extensional flow, in which the differentiation between crystalline and amorphous components is substantially weakened. The present investigation probes the long-range coherence of the macromolecular order with atomic force microscopy (AFM) with molecular-level resolution. The AFM findings support the earlier studies and reveal a remarkable level of long-range coherence in the chain direction with few regions of imperfection — consisting mostly of isolated molecular kinks, flip-over of molecules and gradual coherent twists, but no readily discernible phase-separated amorphous layers. These structural characteristics are consistent with the radical weakening of small-angle X-ray scattering images and the high level of hexagonal coordination of molecules in the stretched 'amorphous' material, which was revealed by X-ray pole figures.

(Keywords: high-density polyethylene; quasi-single-crystal texture; atomic force microscopy)

INTRODUCTION

The mechanism of plastic deformation of semicrystalline polymers, and particularly that of high-density polyethylene (HDPE), has been of interest since the pioneering experiments of Peterlin[1]. Plastic deformation is difficult to study because of the complex spherulitic morphology of the starting semicrystalline material. In the melt-crystallized material, the spherulitic structure is made up of domains of thin and long, plate-like lamellar crystallites separated by non-crystalline interlamellar regions. While the structure of the crystalline component is readily amenable to definitive study, the structure of the amorphous component has been a subject of considerable controversy. The most enlightening account of the constitution of the amorphous component has been given recently by Mandelkern[2], based largely on his own extensive research. According to Mandelkern's conclusions, the amorphous component in the spherulitic polymer consists of a distinct interphase material layer bordering on the crystalline lamellae and a liquid-like central core. A point of principal importance in the structure of the initial spherulitic material is that, in the solid state, characteristic features of the random-coil conformation of the molecules existing previously in the melt are preserved. This rules out any significant occurrence of chain folding in the crystallization of the lamellae. Furthermore, the multitude of experimental probes reveal little detectable structural order in the initial state of the non-crystalline component. Thus, one can assume that the non-crystalline component is predominantly amorphous. At the same time, the crystalline component is relatively defect-free in the initial state.

Argon and coworkers have recently performed an extensive series of experiments on HDPE deformed to very large strains in plane-strain compression[3], uniaxial compression[4] and simple shear[5]. These experiments have demonstrated that, in the early phases of plastic deformation, typically up to an equivalent strain of 0.4, a substantial portion of the strain is derived from the amorphous component. This component is above its T_g at room temperature and behaves in an almost rubbery manner — with much of the early strain being recoverable upon unloading[6]. With increasing deformation, the amorphous component ceases to deform readily and 'locks'. The subsequent deformation to much larger strains is then derived almost entirely from the crystalline component by processes of crystallographic slip. Experiments have indicated that, in the deformation of the crystalline component, the (1 0 0)[0 1 0] is the overwhelmingly preferred chain slip system, which has the lowest slip resistance. This is followed by the (1 0 0)[0 0 1] chain slip system, and to a lesser extent the

*To whom correspondence should be addressed. Present address: Faculty of Chemical Technology, University of Twente, PO Box 217, NL-7500 AE Enschede, The Netherlands

(1 0 0)[0 1 0] transverse system on the best slip plane[6]. All other slip systems, and the various shear transformations of twinning and martensitic shears, were found to make only negligible contributions to the overall deformation.

The plane-strain compression experiment (which is perhaps the least complicated deformation mode) has shown that, in the development of large strain and the associated texture evolution, an important hurdle is overcome at an equivalent strain of 1.14. Here the highly elongated crystalline lamellae apparently begin to undergo fragmentation by multiple pinch-off, resulting in the establishment of a new long period of layered crystalline lamellae and planar amorphous zones, structured across the principal direction of molecular orientation. A qualitatively similar process that occurs in uniaxial tension in the presence of extensive local cavitation was termed 'micro-necking' by Peterlin[1]. Further deformation (in plane-strain compression) then results in a quasi-single-crystalline texture at a principal extensional strain of about 1.86, where the (1 0 0) slip planes have rotated to become normal to the principal compression direction, and the (0 1 0) planes become parallel to the constraining walls of the channel die in which the plane-strain compression is achieved. During all this, the molecular *c* direction, [0 0 1], becomes substantially parallel to the principal flow direction. Recent X-ray deconvolution experiments of Bartczak *et al.*[7] have revealed that the quasi-single-crystalline texture of plane-strain (channel die) compression is not limited only to the crystalline component of the material, but is also prevalent to a very high degree in the amorphous component. At this overall strain of 1.86, the amorphous component shows a hexagonal symmetry, aligned accurately with the nearly hexagonal symmetry of the orthorhombic crystalline component. This strongly suggests that the molecular segments of the amorphous component are continuous with their counterparts in the crystalline component, and that the oriented and restructured lamellae impose their crystal structure on the amorphous component — at least in the planes perpendicular to the aligned axis of molecules. Bartczak *et al.*[7] have found no crystal-like order in the direction of molecular alignment in the transversely ordered amorphous component. This observation, and the earlier findings of Galeski *et al.*[3] on the substantial weakening of the intensity and the broadening of the angular width of the small-angle X-ray scattering (SAXS) patterns of this quasi-single-crystalline texture, implies that a long-range coherence in the principal molecular orientation parallel to the flow direction is established.

In this paper we report on the results of an atomic force microscopy (AFM) study with molecular-level resolution of this quasi-single-crystal textured HDPE — resulting from plane-strain compression to an equivalent strain of 1.86. We have already reported on the use of this highly textured material to measure plastic-shear resistances of specific crystallographic slip systems[6]. Results of other studies using similarly textured nylon-6 to measure the kinetics of chain slip and its implications regarding long-range motion of dislocations in the crystalline component will be reported elsewhere[8,9]. Clearly, the degree of perfection of the quasi-single-crystalline material and its long-range coherence also have important implications for the spatial topology of molecules in the starting spherulitic structure to which it relates, through a series of continuous shape transformations[10-12].

EXPERIMENTAL DETAILS

Morphological texture evolution by SAXS

The most effective method of probing the morphological alterations in a semicrystalline polymer is through the use of small-angle X-ray scattering (SAXS). The particular method of SAXS that was used in the present study has been discussed in detail by Galeski *et al.*[3] and will not be repeated here.

Atomic force microscopy (AFM)

The atomic force microscope, invented in 1986[13] (for a general review, see ref. 14), has been successfully used to visualize and study the surface structure of ordered solid polymers from a true molecular perspective[15-18] on the ångström scale. The AFM is capable of visualizing as few as several dozen atoms or groups of atoms at preselected locations of the sample surface, and thus allows one to obtain *local* information about the molecular organization of solid materials.

Previously, we demonstrated that AFM has the potential to address questions related to the short-range vs. long-range order and disorder, and the orientation mechanism in anisotropic polymers[17-19]. Here we apply the AFM technique to exploring the molecular structure of the oriented high-density polyethylene (HDPE) referred to in the 'Introduction'. We report on results obtained on specimens with a quasi-single-crystalline structure obtained by plane-strain compression flow to an equivalent strain of 1.86 using a channel die. These AFM experiments were performed in order to explore the degree of long-range coherence in aligned molecules, and to clarify the orientation mechanism in these materials. It is anticipated that the AFM images will help to clarify the nature of topological transformations that have connected this final state to the starting spherulitic state. Results of our earlier AFM work showed that both the *ac* and the *bc* crystal facets of the orthorhombic crystal structure of polyethylene can be imaged on the surface of cleaved samples of oriented ultra-high-molecular-weight polyethylene (UHMWPE)[18]. Samples with a high degree of anisotropy were obtained in that study by gel drawing[20]. A conclusion drawn from this earlier work was that no significant molecular relaxation occurred at the free surface of the microfibrils of the oriented specimens. Thus, results of AFM studies at free surfaces of HDPE can be used to draw conclusions about the molecular organization in the bulk.

Samples for AFM study were prepared from rectangular blocks of quasi-single-crystalline HDPE ($\varepsilon_e = 1.86$) at ambient temperatures by using a Sorvall MT6000 ultramicrotome with glass knives. Samples used were identical with those described in ref. 3 at the corresponding draw ratio. After the removal of a few sections from the surfaces of the specimens, the residual samples were studied by AFM. Images were taken in air at room temperature using a NanoScope II (Digital Instruments) instrument with an 'A-type' scanner. NanoProbe 100 μm size triangular Si_3N_4 microcantilevers with short, thin legs were used. Imaging was performed in the 'constant-

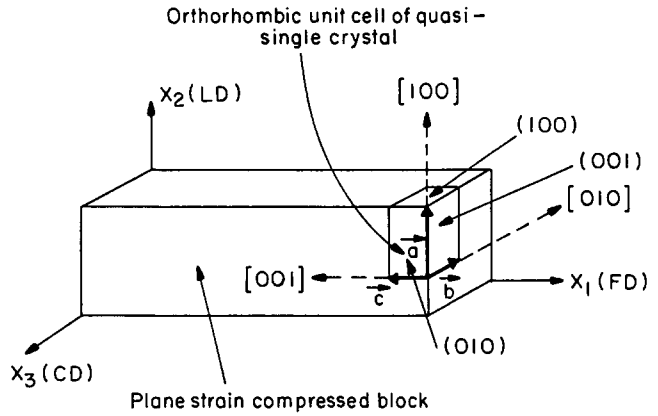

Figure 1 Geometry of the plane-strain compression flow field and how it relates to the quasi-single-crystalline texture of orthorhombic HDPE strained to $\varepsilon_e = 1.86$

height' mode, and raw data were obtained with the low-pass filter set to 1 and the high-pass filter set to 4. For distance calibration, images of muscovite mica were used with 'atomic' resolution.

EXPERIMENTAL RESULTS

Morphological texture evolution by SAXS

The development of morphological texture in plane-strain compression was discussed in full detail elsewhere by Galeski *et al.*[3]. It was shown that, at an equivalent strain of 1.86, an ultimate texture with characteristics typical of a quasi-single-crystalline material is achieved. The associated computer simulation of this development, up to the morphological restructuring that occurs (at $\varepsilon_e = 1.14$) by widespread lamella pinch-off, was discussed by Lee *et al.*[11]. We reproduce here only the essential elements of the SAXS results of Galeski *et al.*[3] that are necessary to understand the results of the present AFM experiments.

Figure 1 shows the overall geometry of the plane-strain compression flow field applied in this study. The Cartesian axes are labelled by x_1, x_2 and x_3 respectively. In the reference system used, x_1 is parallel to the principal direction of the extensional flow, referred to as the *flow direction* (FD). The direction of compression loading, referred to as the *loading direction* (LD), is parallel to x_2. Finally, x_3 is parallel to the normal direction of the plane of the channel wall. The rigid channel wall constrains the deformation to plane-strain flow, and thus the direction marked by x_3 is referred to as the *constraint direction* (CD). The ultimate quasi-single-crystalline texture achieved with a compression ratio of 6.44 ($\varepsilon_e = 1.86$) shows a high degree of alignment of the orthorhombic axes ***c*** ([0 0 1]), ***a*** ([1 0 0]) and ***b*** ([0 1 0]) with the deformation field axes x_1 (FD), x_2 (LD) and x_3 (CD). This conclusion is reached from the WAXS pole figures of Galeski *et al.*[3] (their figure 14).

Figures 2a–2d show the development of the SAXS patterns obtained at different stages of the plane-strain compression in the x_3 (CD), x_2 (LD) and x_1 (FD) directions, respectively. *Figure 2a* displays results measured on the undeformed spherulitic material. *Figure 2b* is the SAXS pattern of the material strained to a compression ratio (CR) of 2.5 ($\varepsilon_e = 0.92$) before the morphological restructuring by lamella pinch-off occurs. *Figure 2c* represents the SAXS intensity of the material strained to $CR = 3.13$ ($\varepsilon_e = 1.14$) just after the major morphological restructuring by lamella pinch-off occurs, initiating the establishment of the new long period. *Figure 2d* illustrates the SAXS intensity of the ultimate quasi-single-crystalline texture at $CR = 6.44$ ($\varepsilon_e = 1.86$). We wish to point out the existence of the completely isotropic SAXS patterns of the starting state (*Figure 2a*), and the very weak SAXS pattern in the LD direction of the final quasi-single-crystalline texture at $\varepsilon_e = 1.86$[3] (*Figure 2d*). The 'two-point' diffuse SAXS pattern in the LD direction in *Figure 2d* defines the nature of the planar stack-like new long period. Comparison of this pattern with the corresponding much stronger pattern in *Figure 2a* indicates that: (a) the wavelength of the new long period is only about 60% of that of the initial state, (b) the range in the long-period spacing in the final state is nearly twice

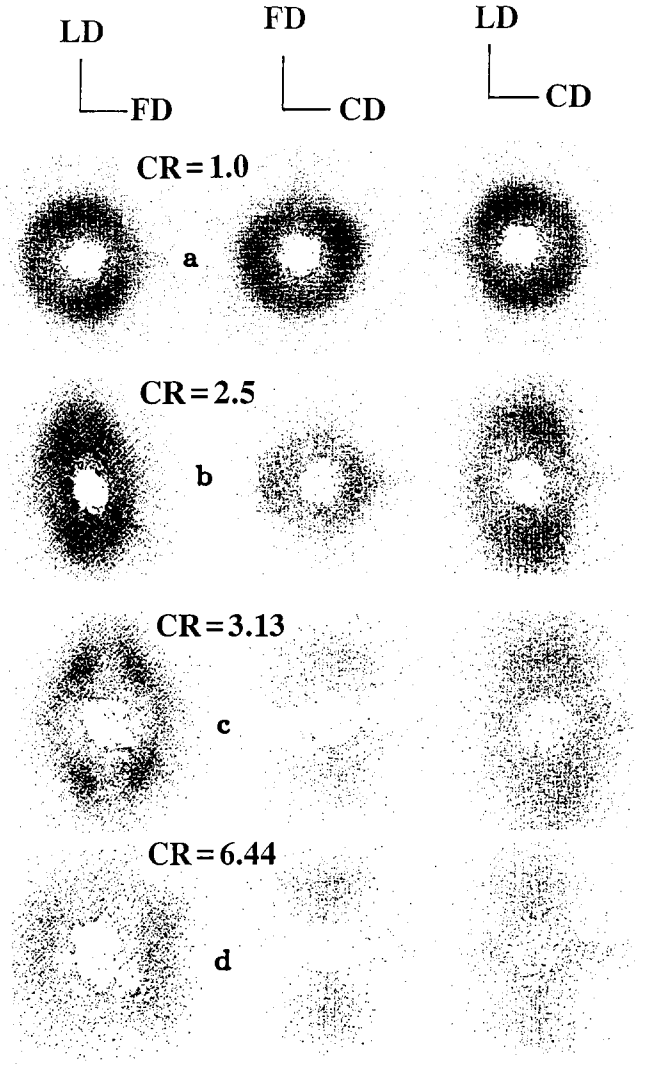

Figure 2 Small-angle X-ray scattering patterns: (a) the initial isotropic spherulitic material; (b) material strained to a compression ratio (CR) of 2.5 ($\varepsilon_e = 0.92$), before the morphological restructuring by widespread lamella pinch-off; (c) CR of 3.13 ($\varepsilon_e = 1.14$), immediately after the morphological restructuring by widespread lamella pinch-off; and (d) CR of 6.44 ($\varepsilon_e = 1.86$), the final quasi-single-crystalline state with the new faint long period

Figure 3 A low-magnification scan ($1.1 \times 1.1\ \mu m^2$) of the x_2 plane, showing coarse fibrillar microstructure

as large as that in the initial state, and (c) the total scattering intensity in the final state is very much weaker. All of this signifies a strong dispersal and reduction of the clear definition of the amorphous component. In anticipation of the AFM results presented below, we interpret these changes in the SAXS pattern as the establishment of long-range coherence in the chain direction x_1 (FD).

AFM observations of molecular-level structure

The AFM observations were made on the two surfaces perpendicular to the x_2 and x_3 axes, which in the perfect quasi-single crystal should refer to the (1 0 0) and (0 1 0) planes of the orthorhombic crystal structure, or, alternatively, to the *bc* and *ac* planes, respectively.

A typical AFM scan of a $1.1 \times 1.1\ \mu m^2$ area of the cleaved surface of an oriented specimen with a normal vector $\boldsymbol{x}_2$ (the expected *bc* plane) is shown in *Figure 3*. On this scan, the $\boldsymbol{x}_1$ direction is approximately parallel to the diagonal defined by the top left and bottom right corners of the nanograph. This and similar micrometre-scale AFM images of the other face with normal vector $\boldsymbol{x}_3$ revealed a morphology of well aligned microfibrils with a typical fibrillar diameter in the range of ca. 50–150 nm. This observation confirms earlier light optical and electron microscopy results of Galeski *et al.*[3].

Nearly 100 AFM images with molecular-level resolution were obtained on the two lateral planes of compressed samples with normal vectors $\boldsymbol{x}_2$ and $\boldsymbol{x}_3$, respectively. All the imaged crystal facets included the crystallographic *c* direction, which always stood out clearly. Chain–chain packing distances were determined from the two-dimensional autocorrelation patterns of the nanographs. The values obtained allowed us to identify the crystal facets captured on the AFM scans. Interestingly, both the *a* and *b* crystallographic repeat lengths were observed in both sample faces. It must be stressed, however, that the overwhelming majority of the AFM nanographs captured in the plane with the $\boldsymbol{x}_2$ normal vector corresponded to the crystallographic *bc* facet, while AFM observations in the plane with the $\boldsymbol{x}_3$ normal vector showed the dominating presence of the *ac* facet. These observations are consistent with the pole figures, which — although exhibiting single-crystal-like textures — show appreciable intensities for the (2 0 0) plane in the constraint direction, and for the (0 2 0) plane in the loading direction[3].

Typical nanographs showing the polymer chains in the two planes mentioned in the previous paragraph are displayed in *Figures 4* and *5*, respectively. The grey scale on the photographs is proportional to the cantilever deflection of the AFM probe. The 'ridges' correspond to the images of individual macromolecules. The expected *bc* crystal facet captured in the plane with the $\boldsymbol{x}_2$ normal

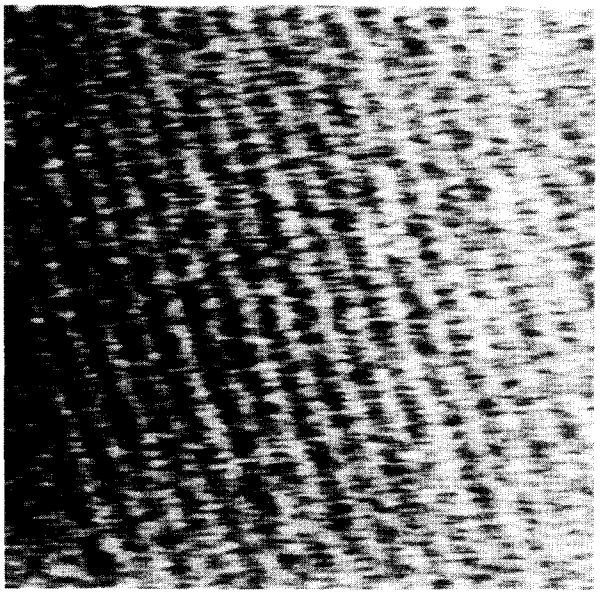

Figure 4 High-resolution scan ($8 \times 8\ nm^2$) of the x_2 plane in an area with the *bc* crystal facet ($|\boldsymbol{b}| = 4.60$ nm)

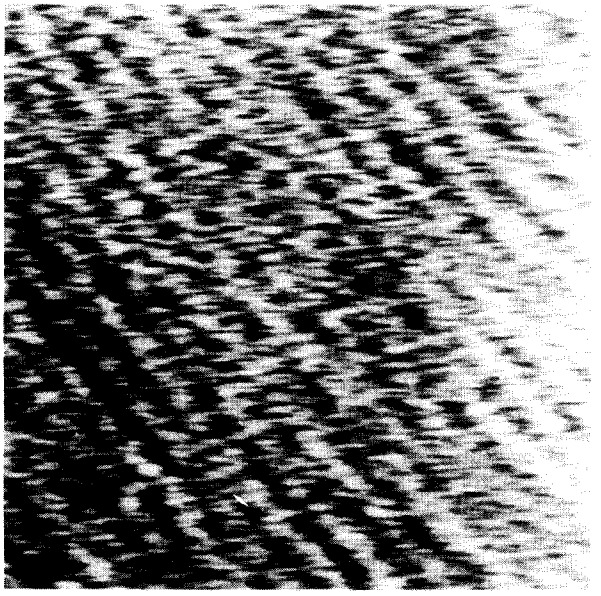

Figure 5 High-resolution scan ($12 \times 12\ nm^2$) of the x_3 plane in an area with the *ac* crystal facet ($|\boldsymbol{a}| = 7.39$ Å)

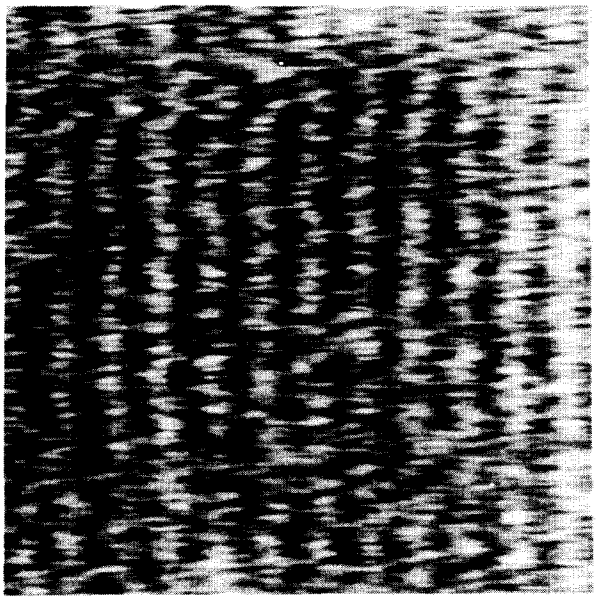

Figure 6 High-resolution nanograph (3×3 nm^2) obtained by scanning parallel to the molecular orientation (horizontal direction) on the x_2 plane. The repeat distance along the chain direction is $|c| = 2.50$ Å

vector is shown in *Figure 4* ($|b| = 4.60$ Å). A typical nanograph obtained in the plane with the x_3 normal vector, identified as the expected *ac* crystal facet ($|a| = 7.39$ Å), is captured in *Figure 5*.

Some structure is visible along the chains in all the nanographs shown. In order to resolve this structure better, the samples were rotated such that the chain direction became parallel to the scan direction (i.e. nearly horizontal on the nanographs). Generally, rotation of the sample with respect to the scan direction can help to resolve different details of the macromolecules, as we noted in an earlier communication[21]. A typical corresponding scan is shown in *Figure 6*. While developing this scan, the tip moved in the 'grooves' between the chains and on 'top' of the chains. The ridges in the figure correspond to features made up by the methylene groups of neighbouring macromolecules, and are perpendicular to the (horizontal) chain direction. Thus, the chains are in register in the *c* direction, as expected, for the crystalline component of the quasi-single crystal. In this nanograph, however, the chains themselves are not resolved. The crystallographic *c* repeat unit was determined from the distance between the ridges, and a value of $|c| = 2.50$ Å was obtained. This is in excellent agreement (to within the experimental error of ca. $\pm 8\%$) with the expected repeat length of $|c| = 2.54$ Å. It is worth noting that simultaneous resolution of both the polymer chains and the methylene groups along the chains has already been achieved in extruded HDPE[16] and fibres of ultra-high-molecular-weight polyethylene, drawn from gel[22].

AFM search for long period

In order to check whether ordered regions in the oriented samples are separated by amorphous layers, individual chains were followed over domains with sizes typically between 40 and 70 nm. Since it was essential to maintain the resolution typical in nanographs shown in *Figures 4* and *5*, images with a scan size of 10×10 nm^2 were assembled. In this way, longer sections of the chains can be shown by putting together high-resolution images similar to a 'jig-saw puzzle'. The scanned area was shifted between capturing two consecutive images of this 'puzzle' by a distance that was at most equal to the scan size of an individual nanograph. Single chains and features at overlapping areas of two consecutive images can easily be recognized in *Figures 7* and *8*, which were assembled in this manner. *Figure 7* displays a spot of ca. 40 nm total length in the chain direction, obtained from the x_3 plane. Another image obtained in the same plane but at a different region is shown in *Figure 8*, exhibiting a section of ca. 50 nm domain length. Both montages capture the

Figure 7 Montage of six high-resolution (10×10 nm^2) scans on the x_3 plane in the region of the expected *ac* crystal facet. Over the entire length of 38 nm along the chain direction, no readily discernible amorphous region could be found

Figure 8 Montage of five high-resolution ($10 \times 10\ nm^2$) scans on the x_3 plane in a different region of the expected *ac* crystal facet. Over the length of 50 nm along the chain direction, no readily discernible amorphous region could be found

expected dominant *ac* crystallographic facets on the x_3 plane. The corresponding SAXS pattern for these images is one on the left in *Figure 2d* showing elongated sets of spots typical of this orientation. In this case the stacking of the lamellae and the amorphous layers is expected to have a periodically sheared shape, as was discussed in detail by Song *et al.*[23]. Four other 'jig-saw puzzles', similar to those shown in *Figures 7* and *8*, were assembled. All six montages studied showed quite similar features. It is apparent that the chain packing is disordered in certain areas. Twisted chains (flip-over interchanges), paracrystalline disorder and entanglements can be found in several locations of the images. There are also gradual coherent twists in blocks of molecules that result in *ac* facets on the x_2 plane and *bc* facets on the x_3 plane. It must be emphasized that our observations show no readily discernible indication of a well delineated two-phase system with alternating amorphous and crystalline layers. The weak SAXS images of the type given in *Figure 2d* for the LD direction suggest that a long period of ordered domains separated by amorphous layers with a ca. 260 Å characteristic separation might be present in the compressed samples. This suggested structure was not apparent by our direct visualization of the polymer chains from a true molecular perspective, indicating only that the amorphous material must be well diffused and not sharply 'phase-separated'. This confirms the suspected long-range transverse coherence in the chain direction, which was concluded from the deconvoluted pole figures of the amorphous component obtained recently by Bartczak *et al.*[7].

DISCUSSION AND CONCLUSIONS

Results of AFM and SAXS measurements were used in this work to investigate the long-range structural coherence of macromolecular order in highly textured HDPE obtained by plane-strain compression. There was no indication of a well delineated amorphous component found in the present AFM study. This result is supported by the recent discovery by Bartczak *et al.*[7] of a hexagonal symmetry transverse to the chain direction in the amorphous material (obtained from pole figures constructed from the deconvolution of the diffracted intensities of the amorphous material). The study of Bartczak *et al.*[7] indicates the existence of lateral registry of the hexagonal symmetry of the oriented amorphous material with the orthorhombic structure of the aligned crystalline layers. X-ray pole figures revealed a quasi-single-crystalline texture of the highly oriented material. All these results consistently reinforce the existence of a remarkably well oriented material with long-range coherence in the chain direction, parallel to the principal (FD) direction of the extensional flow.

First, it is clear that such a quasi-single-crystalline material is ideally suited to study the kinetics of the mechanisms of chain slip, as has already been done by Lin and Argon[9] on similarly prepared nylon-6. The important implications of long-range mobility of dislocations in such material must be noted.

Secondly, a point of perhaps more profound nature is to note the topological connection of this quasi-single-crystalline material with long-range coherence to its initial spherulitic state from which it was obtained by an uninterrupted series of shape transformations. The recent successful computer simulations of the evolution of deformation-induced textures in HDPE by Parks and coworkers[10,24,25], using sandwich elements of adhered crystalline lamellae and amorphous regions (capable of undergoing orientation hardening), can be taken as sufficient verification of the assumed topologically uninterrupted shape transformations. Such transformations connect the initial spherulitic morphology to the structure

of the final quasi-single-crystalline material. Clearly, such a series of transformations is most compatible with an initial random-coil conformation of individual macromolecules treading through crystalline lamellae in the initial spherulitic material. This is clearly in conflict with any substantial frequency of chain folding in the lamellae of the initial spherulitic state.

ACKNOWLEDGEMENTS

The Toronto team would like to thank Dr Daniel Snétivy for his most valuable help with the AFM experiments. The financial support of the Natural Sciences and Engineering Research Council of Canada and the Ontario Centre for Materials Research is gratefully acknowledged. H. Schönherr thanks the 'Deutscher Akademischer Austauschdienst' for financial support in the form of an overseas student exchange award. The research of A. S. Argon has been supported up to the present by a DARPA URI programme under ONR Contract No. N00014-86-K-0768.

REFERENCES

1 Peterlin, A. *J. Mater. Sci.* 1971, **6**, 490
2 Mandelkern, L. in 'Crystallization of Polymers' (Ed. M. Dosiére), NATO-ASI Series C, Vol. 405, Kluwer Academic, Brussels, 1993, p. 25
3 Galeski, A., Bartczak, Z., Argon, A. S. and Cohen, R. E. *Macromolecules* 1992, **25**, 5705
4 Bartczak, Z., Cohen, R. E. and Argon, A. S. *Macromolecules* 1992, **25**, 4692
5 Bartczak, Z., Argon, A. S. and Cohen, R. E. *Polymer* 1994, **35**, 3427
6 Bartczak, Z., Argon, A. S. and Cohen, R. E. *Macromolecules* 1992, **25**, 5036
7 Bartczak, Z., Galeski, A., Argon, A. S. and Cohen, R. E. *Polymer* in press
8 Argon, A. S., Lin, L. and Vancso, G. J. in 'Deformation, Yield and Fracture of Polymers', Institute of Materials, London, 1994, p. 21/1
9 Lin, L. and Argon, A. S. *Macromolecules* 1994, **27**, 6903
10 Lee, B. J., Parks, D. M. and Ahzi, S. *J. Mech. Phys. Solids* 1993, **41**, 1651
11 Lee, B. J., Argon, A. S., Parks, D. M., Ahzi, S. and Bartczak, Z. *Polymer* 1993, **34**, 3555
12 Argon, A. S., Bartczak, Z., Cohen, R. E., Galeski, A., Lee, B. J. and Parks, D. M. in 'Oriented Polymer Materials' (Ed. S. Fakirov), Hüthig and Wepf, Basel, in press
13 Binnig, G., Quate, C. F. and Gerber, C. *Phys. Rev. Lett.* 1986, **56**, 930
14 Sarid, D. 'Scanning Force Microscopy with Applications to Electric, Magnetic, and Atomic Forces', Oxford University Press, Oxford, 1991; Bonnell, D. A. (Ed.) 'Scanning Tunneling Microscopy and Spectroscopy, Theory, Techniques and Applications', VCH, Weinheim, 1993
15 Marti, O., Ribi, H. O., Drake, B., Albrecht, T. R., Quate, C. F. and Hansma, P. K. *Science* 1988, **239**, 50
16 Magonov, S. N., Quarnstöm, K., Elings, V. and Cantow, H.-J. *Polym. Bull.* 1991, **25**, 689
17 Snétivy, D., Vancso, G. J. and Rutledge, G. C. *Macromolecules* 1992, **25**, 7037
18 Snétivy, D., Yang, H. and Vancso, G. J. *J. Mater. Chem.* 1992, **2**, 891
19 Snétivy, D. and Vancso, G. J. *Polymer* 1994, **35**, 461
20 Smith, P. and Lemstra, P. J. *Colloid Polym. Sci.* 1980, **258**, 891; Smith, P., Lemstra, P. J. and Booij, H. C. *J. Polym. Sci., Polym. Phys. Edn.* 1981, **19**, 877
21 Snétivy, D., Guillet, J. E. and Vancso, G. J. *Polymer* 1993, **34**, 429
22 Magonov, S. N., Sheiko, S. S., Deblieck, R. A. C. and Möller, M. *Macromolecules* 1993, **26**, 1380
23 Song, H. H., Argon, A. S. and Cohen, R. E. *Macromolecules* 1990, **23**, 870
24 Parks, D. M. and Ahzi, S. *J. Mech. Phys. Solids* 1990, **38**, 701
25 Ahzi, S., Parks, D. M. and Argon, A. S. in 'Computer Modeling and Simulation of Manufacturing Processes' (Eds. B. Singh, Y. T. Im, I. Hague and C. Altan), Book No. G00552, ASME, New York, 1990, MD-20, p. 287